Rhodohalobacter sulfatireducens sp. nov., isolated from a marine solar saltern

Yu-Sheng Wang
Shandong University at Weihai
Yu-Yan Yue
Shandong University at Weihai
Yi-Lin Bai
Shandong University at Weihai
Xu-Yang Zhang
Shandong University at Weihai
Shuo Wang
Shandong University at Weihai
Zong-Jun Du (duzongjun@sdu.edu.cn)
Shandong University https://orcid.org/0000-0002-7886-5667

Research Article

Keywords: Rhodohalobacter, 16S rRNA gene, phylogenetic analysis

Posted Date: March 22nd, 2022

DOI: https://doi.org/10.21203/rs.3.rs-1454253/v1

Abstract

A novel Gram-stain-negative, oxidase-positive, catalase-positive, non-motile, facultatively anaerobic, and rod-shaped bacterium, designated WB101^T, was isolated from a marine solar saltern located in Wendeng, PR China. Growth occurs at 25–42°C (optimum, 35–37°C), 1.0–11.0% (w/v) NaCl (optimum, 5.0–6.0%), and pH 7.0–8.5 (optimum, 7.5–8.0). Analysis based on the 16S rRNA gene sequences revealed that WB101^T shared high level of sequence similarity with *Rhodohalobacter barkolensis* 15182^T (93.5%), *Rhodohalobacter halophilus* JZ3C29^T (93.2%), and '*Rhodohalobacter mucosus*' 8A47^T (92.1%). Strain WB101^T formed an evident species-level clade within the genus *Rhodohalobacter* in both phylogenetic and phylogenomic topologies. The draft genome of strain WB101^T is 5,104,032 bp in size, and the G + C content is 42.0 mol%. The genomic sequencing yields 138 contigs with an N50 value of 123,641 and a coverage depth of 275.0 ×. The strain encodes a complete assimilatory sulfate reduction pathway. The sole respiratory quinone was menaquinone 7. The dominant cellular fatty acid (≥ 10%) was iso-$C_{15:0}$. The polar lipid profile of the novel isolate included diphosphatidylglycerol, phosphatidylglycerol, phosphatidylcholine, and phosphatidylethanolamine. Based on its phylogenetic, physiological, and biochemical properties, strain WB101^T should be classified as a novel species of the genus *Rhodohalobacter*, for which the name *Rhodohalobacter sulfatireducens* sp. nov. is proposed. The type strain is WB101^T (= KCTC 92204^T = MCCC 1H00518^T).

Introduction

The genus *Rhodohalobacter*, belonging to the family *Balneolaceae* (Xia et al. 2016), was firstly established by Xia et al. (2017). At the time of writing, there are two valid species: *Rhodohalobacter halophilus* (Xia et al. 2017) and *Rhodohalobacter barkolensis* (Han et al. 2018), and one unvalidated species: '*Rhodohalobacter mucosus*' (Wang et al. 2021), according to the List of Prokaryotic names with Standing in Nomenclature (LPSN) (https://lpsn.dsmz.de). All above were isolated from saline environments, including salterns and saline lakes.

Sulfur metabolism occurs depending on different organisms in the environment. Microorganisms can involve sulfur in their metabolism, both in oxidized and reduced states (Carbonero et al. 2012). In the process of assimilatory sulfate reduction (ASR), sulfate is reduced to sulfide, and then the production participates synthesis of organic compounds, such as sulfur amino acids. Compared with dissimilatory sulfate reduction, ASR is a more favourable metabolic pathway to bacteria because no toxic sulfide is produced during this process.

In this study, we propose a novel species with the polyphasic taxonomy performed, named *Rhodohalobacter sulfatireducens* sp. nov. The cells can provide a vessel for ASR. This study increases the members of the genus *Rhodohalobacter* and enriches the research directions of the study on assimilatory sulfate-reducing bacteria.

Material And Methods

Isolation and maintenance conditions

Coastal sediment was used as a source of bacterial isolation, which was sampled from a marine solar saltern of Wendeng, PR China (122° 1' 45" E, 36° 59' 38" N) in November 2020. The sample was serially diluted to 10^{-4} times with sterilized seawater, and 0.1 mL aliquots of each dilution were spread onto marine agar 2216 (MA; BD). Plates were incubated at 33°C for two weeks. Finally, a tiny, reddish, convex, circular, and regular-edged colony was isolated, purified, and subsequently designated as strain WB101^T. For long-term storage, the strain was stored at -80°C in sterile 15% (v/v) glycerol supplemented with 5.0% (w/v) NaCl. '*Rhodohalobacter mucosus*' 8A47^T, *Rhodohalobacter halophilus* JZ3C29^T (both isolated and published by our laboratory), and *Rhodohalobacter barkolensis* MCCC 1K03442^T (obtained from Marine Culture Collection of China, MCCC) were collected as related type strains.

Phylogenetic and phylogenomic analyses

The sequence of the 16S rRNA gene was amplified by PCR with the universal primers 27F and 1492R (Liu et al. 2014). After electrophoresis, the purified PCR product was regained by agarose gel DNA extraction kit (TaKaRa), ligated into the pMD19-T vector (TaKaRa), and cloned according to the manufacturer's instructions. Sequencing was performed by Tsingke Biotechnology Co., Ltd. (Qingdao, PR China) using the universal primers M13F and M13R. The 16S rRNA gene sequence annotated from the genome sequences was submitted to GenBank databases. Similar sequences were searched using the BLAST algorithm (https://www.ncbi.nlm.nih.gov). The EzBioCloud's identification service (https://eztaxon-e.ezbiocloud.net) (Kim et al. 2012) was used to determine the similarity values among the sequences. Genomic DNA was extracted and purified using a bacterial genomic DNA extraction kit (TaKaRa) following the manufacturer's instructions. The draft genome was sequenced by Novogene Biotechnology Co., PR China, using the Illumina HiSeq platform (Illumina, San Diego, CA, USA). Raw sequencing reads were assembled by ABySS v. 2.0.2 (http://www.bcgsc.ca/platform/bioinfo/software/125 abyss) (Simpson et al. 2009).

Phylogenetic trees were performed using MEGA 7 (Kumar et al. 2016) with neighbour-joining (NJ) (Saitou and Nei 1987) method based on complete 16S rRNA gene retrieved from the genome sequences. Maximum-parsimony (MP) (Fitch 1971) and maximum-likelihood (ML) (Felsenstein 1981) methods were used to confirm the phylogenetic status of strain WB101^T. Evolutionary distances were calculated with Kimura two-parameter model (Kimura 1980). Bootstrap analysis with 1,000 replications was used to evaluate tree topologies.

To detect the taxonomic status of strain WB101^T at the genomic level, a phylogenomic tree based on genomes inferred bac120 marker set was constructed using GTDB (Genome Taxonomy Database) (https://gtdb.ecogenomic.org) (Chaumeil et al. 2019). The average nucleotide identity (ANI) values (including OrthoANIu, ANIb, ANIm, and TETRA values) were performed by online calculator EzGenomes

(http://www.ezbiocloud.net/tools/ani) (Yoon et al. 2017) and JspiecesWS (http://jspecies.ribohost.com/jspeciesws) (Richter et al. 2016). The digital DNA-DNA hybridization (dDDH) values were calculated using GGDC (ggdc.dsmz.de) (Meier-Kolthoff et al. 2022). As additional taxonomic references, the average amino acid identity (AAI) (Rodriguez-R and Konstantinidis 2014) and the percentage of conserved proteins (POCP) (Qin et al. 2014) between related genomes were determined by an AAI and POCP calculator (github.com/2015qyliang/POCP).

Genomic analyses

Secondary metabolite clusters were identified by antiSMASH (antismash.secondarymetabolites.org) (Medema et al. 2011). Genome annotation was performed using the RAST server (rast.nmpdr.org) (Aziz et al. 2008) and KEGG pathway annotation (www.kegg.jp) (Kanehisa et al. 2016).

Morphological, physiological, and biochemical analyses

The morphological and physiological features of strain WB101^T were examined after incubation at 37°C on MA for three days. A scanning electron microscope (Nova NanoSEM 450; FEI) was used to observe the cell morphology. A late exponential phase culture (three days, according to growth curves in Supplementary Fig. S1) in marine broth 2216 (MB; BD) was collected for fixation with 2.5% glutaraldehyde solution preserved under 4°C. Then, gradient dehydration was performed with 50%, 70%, 80%, 90%, and 100% ethanol before observation. Gram-staining was performed using a Gram-stain kit (Hopebio) according to the manufacturer's instructions. Motility was examined with 3.0% (w/v) NaCl solution according to the hanging-drop method (Bowman 2000). Gliding was assessed using MB supplemented with 0.3% (w/v) agar according to the method described by Bernardet et al. (2002). Oxidase activity was tested using an oxidase reagent kit (bioMérieux) according to the manufacturer's instructions. Catalase activity was determined by the visible bubble production in a 3% (v/v) H_2O_2 solution.

The effects of different growth temperatures were tested at 4, 15, 20, 25, 28, 30, 33, 35, 37, 40, 42, and 45°C on MA. Growths under different NaCl concentrations were assessed using a modified MA (1 g yeast extract L^{-1}, 5 g peptone L^{-1}, 0.1 g ferric citrate L^{-1}, and 18 g agar L^{-1}), prepared with artificial seawater (0.32% $MgSO_4$, 0.12% $CaCl_2$, 0.07% KCl, and 0.02% $NaHCO_3$, all w/v). NaCl concentrations were adjusted from 0 to 13.0% (w/v) at an interval of 1.0%, respectively. To test the interference of pH on growth, MB was adjusted to different pH levels with the additional buffers (Sangon): MES (pH 5.5 and 6.0), PIPES (pH 6.5 and 7.0), HEPES (pH 7.5 and 8.0), Tricine (pH 8.5), and CAPSO (pH 9.0 and 9.5) at concentrations of 20 mM. The effects of temperature, NaCl tolerance, and pH on the growth were recorded every 12 h in a 96-hour-incubation (determined by growth curve) featuring visible colonies or optical density at 600 nm wavelength (OD_{600}). Anaerobic growth was determined at 37°C for three weeks on modified MA with or without 0.1% (w/v) KNO_3 in an anaerobic incubation system. The ability of nitrate-reduction was evaluated following the description from Cowan and Steel (1974). H_2S production was tested according to lead acetate papers (Wang et al. 2012) and producing black precipitates in triple-sugar iron agar (TSI; BD). Hydrolysis of DNA, starch, casein, alginate, carboxymethyl cellulose (CMC), and esters, including

Tweens 20, 40, 60, and 80, were investigated according to the methods of Smibert and Krieg (1994). Susceptibility to antibiotics was assessed as described by the Clinical and Laboratory Standards Institute (CLSI) (2012) on MA at 37°C. Measuring the size of the inhibition zones generated by different drug-sensitive papers was performed until visible bacterial lawns were observed.

Other physiological and biochemical characteristics were tested by API 20NE, API ZYM, and API 50CH (all from bioMérieux). The oxidising potential of strain WB101^T for various carbon sources was assessed using Biolog GEN III. All the API and Biolog tests were performed with three related type strains ('*R. mucosus*' 8A47^T, *R. barkolensis* MCCC 1K03442^T, and *R. halophilus* JZ3C29^T), according to the manufacturer's instructions, except that the NaCl concentration was adjusted to 5.0%, 3.0% and 10.0% (w/v), respectively, which were the optimal salinities for them.

Chemotaxonomic analyses

To extract respiratory quinones, polar lipids, and fatty acids, cells of the late exponential stage (according to growth curve) of strain WB101^T, and related type strains were harvested and freeze-dried, which were incubated in MB at 37°C by the four quadrants streak method.

Respiratory isoprenoid quinones were extracted from 300 mg cell material and separated into different classes by thin-layer chromatography (TLC) on silica gel. The effective components were removed from the plate relying on the spots and analysed further by using reverse-phase high-performance liquid chromatography (HPLC) according to Kroppenstedt (1982).

Polar lipids were extracted from 100 mg cell material and separated via TLC on silica gel plates (8 × 8 cm, no. 5554; Merck) according to the methods of Tindall et al. (2007). Total lipid materials were detected using molybdatophosphoric acid, and specific functional groups were tested by spray staining reagents (Sigma-Aldrich) on four separate TLC plates, which included phosphomolybdic acid solution (total lipids), molybdenum blue solution (phosphates), *α*-naphthol sulfuric solution (carbohydrates), and ninhydrin (amines).

Fatty acids were extracted from 40 mg cell material and saponified, methylated, and extracted using the standard protocol of the Sherlock Microbial Identification System (MIDI) equipped with Agilent model 6890 N gas chromatograph. Fatty acids with percentages were determined and calculated using the MIS standard software using the TSBA40 database (Buyer 2002).

Results And Discussion

Phylogenetic and phylogenomic analyses

The only complete 16S rRNA gene sequence (1,532 bp) extracted from the draft genome shared 99.9% similarity with the nearly complete sequences (1,505 bp) obtained by conventional Sanger sequencing, which confirms their authenticity. Strain WB101^T exhibited the highest similarity to *Rhodohalobacter*

barkolensis 15182^T (93.5%), followed by *Rhodohalobacter halophilus* JZ3C29^T (93.2%), '*Rhodohalobacter mucosus*' 8A47^T (92.1%), and other validated species of the family *Balneolaceae* (on the edge of or lower than 90.0%). The phylogenetic tree based on the neighbour-joining algorithm showed that strain WB101^T was distinct from *R. halophilus* JZ3C29^T, *R. barkolensis* 15182^T, and '*R. mucosus*' 8A47^T within the genus *Rhodohalobacter* at a high confidence level (Fig. 1), which was also emphasized by additional MP, ML phylogenetic trees.

The draft genome of strain WB101^T was 5,104,032 bp in size, and the DNA G + C content was 42.0 mol%. A total of 138 contigs were assembled from the raw sequences, and the N50 value and coverage depth were 123,641 and 275.0 ×, respectively. The detailed genomic information of strain WB101^T and related type strains are listed in Table 1. Strain WB101^T had a significantly larger genome than the members of the genus *Rhodohalobacter*, though they all share a similar number and contents of tRNAs and G + C mol%.

Table 1
Genomic data that differentiates strain WB101T from related type strains.

Genomic data	**1**	**2[a]**	**3[b]**	**4[c]**
Genome size (bp)	5,104,032	3,908,029	3,597,295	3,122,722
DNA G + C (mol%)	42.0	47.7	42.5	44.4
Number of coding genes	4,233	3,219	3,015	2,727
Number of total pseudo genes	24	9	5	26
Number of tRNAs	38	40	39	38
Number of rRNAs (5S, 16S, 23S)	3, 1, 1	1, 1, 1	2, 1, 1	1, 2, 1
Number of contigs	138	17	7	92
N50 values	123,641	417,940	1,807,017	84,288
Coverage depth	275.0 ×	198.0 ×	544.0 ×	137.9 ×
1, Strain WB101^T; 2, '*R. mucosus*' 8A47^T; 3, *R. barkolensis* 15182^T; 4, *R. halophilus* JZ3C29^T				
Data from: [a], Wang et al. (2021); [b], Han et al. (2018); [c], Xia et al. (2017)				

The OrthoANIu, dDDH, AAI, POCP, and TETRA value between strain WB101^T and '*R. mucosus*' 8A47^T, *R. barkolensis* 15182^T, and *R. halophilus* JZ3C29^T are shown in Table 2. The OrthoANIu values between each of these strains were far lower than 95.0–96.0%, the threshold to identify potential novel species (Richter and Rosselló-Móra 2009). Moreover, the ANIb and ANIm values were all below 90.0%. All the dDDH values were below the threshold value (70.0%) for species delineation, demonstrating that each pair formed deep lineages (Li et al. 2010). TETRA values were lower than 0.99, the threshold for novel

species (Richter and Rosselló-Móra 2009). For the taxonomic boundaries for genera, all the AAI and POCP values between strain WB101^T and each of three related type strains were over 60.0% and 50.0%, respectively, which were argued as genus boundaries (Rodriguez-R and Konstandtinidis 2014; Qin et al. 2014). Additionally, the same taxonomic status shown by phylogenetic trees was also demonstrated by phylogenomic tree based on GTDB (Fig. 2).

Table 2
Phylogenomic value between strain WB101T and related type strains.

Phylogenomic value	**1**	**2**	**3**
OrthoANIu	69.2%	69.5%	69.4%
dDDH	18.5%	17.6%	18.1%
TETRA	0.81	0.93	0.92
AAI	68.0%	68.6%	68.6%
POCP	56.0%	53.4%	52.1%
1, Strain WB101^T vs '*R. mucosus*' 8A47^T; 2, Strain WB101^T vs *R. barkolensis* 15182^T; 3, Strain WB101^T vs *R. halophilus* JZ3C29^T			
The genome of three related type strains from: www.ncbi.nlm.nih.gov			

Genomic analyses

There was no known secondary metabolite cluster identified with high similarity according to antiSMASH. Compared to members of the genus *Rhodohalobacter*, strain WB101^T had a non-ribosomal peptide synthetase cluster (NRPS), which probably suggested an unknown peptide synthesis pathway was encoded by its genome.

Based on the RAST program, the galactosylceramide and sulfatide metabolism pathways with higher copy numbers were encoded by the genome of strain WB101^T than three related type strains. The results of analyses by KOALA (KEGG Orthology And Links Annotation) indicated that strain WB101^T featured in ASR. Reduction of sulfate (+ 6) occurs within cells of strain WB101^T with bifunctional enzyme *CysN*/*CysC* (*cysNC*), sulfate adenylyltransferase subunit 1 and 2 (*cysN* and *cysD*), adenylylsulfate kinase (*cysC*), phosphoadenosine phosphosulfate reductase (*cysH*), and sulfite reductase (*sir*). As an intermediate during this process, PAPS (3'-phosphoadenosine-5'-phosphosulfate) is reduced to sulfite. Then, sulfide is transformed to l-cysteine by *O*-acetyl serine-(thiol)-lyase (Schiff 1979). However, the absence of sulfate permease, encoded by the *cysPUWA* operon, suggests strain WB101^T might not utilise extracellular sulfates (Kushkevych et al. 2020). According to the genomic data from GenBank, the assimilatory sulfate reduction pathways of the genus *Rhodohalobacter* were incomplete in '*R. mucosus*' 8A47^T and *R. barkolensis* 15182^T, and even absent in *R. halophilus* JZ3C29^T. Conversion among polysulfides can be

achieved by sulfhydrogenase subunit gamma, beta, alpha, and delta (*hydG*, *hydB*, *hydA*, and *hydD*) (Ma et al. 2000). Dissimilatory or assimilatory nitrate reduction was incomplete within the genus *Rhodohalobacter* and strain WB101^T, which was testified by the experiment results. Compared to members of the genus *Rhodohalobacter*, strain WB101^T had a more equipped pathway of carbohydrate metabolism, including pentose and glucuronate interconversions, galactose metabolism, amino sugar, and nucleotide sugar metabolism. The ribokinase (*rbsK*) allows cells of strain WB101^T to transform d-ribose 5-phosphate to d-ribose. Phosphatidylcholine (lecithin) could be synthesized by glycerone-*P* with glycerol-3-phosphate dehydrogenase (*gpsA*), acyl phosphate:glycerol-3-phosphate acyltransferase (*plsY*), 1-acyl-sn-glycerol-3-phosphate acyltransferase (*plsC*), lysophosphatidate acyltransferase (*AGPAT1_2*), lysophosphatidic acid acyltransferase / lysophosphatidylinositol acyltransferase (*AGPAT3_4*), lysophosphatidiate acyltransferase (*AGPAT5*), lysocardiolipin and lysophospholipid acyltransferase (*LCLAT1*, *AGPAT8*), lysophospholipid acyltransferase 1/2 (*MBOAT1_2*), lysophospholipid acyltransferase (*LPT1*, *ALE1*), TAG lipase / sterylester hydrolase / phospholipase A2 / LPA acyltransferase (*TGL4*), 1-acylglycerol-3-phosphate *O*-acyltransferase (*LOA1*), phosphatidate cytidylyltransferase (*CDS1*, *CDS2*, *cdsA*), and phosphatidylcholine synthase (*pcs*). In summary, compared to species of the genus *Rhodohalobacter*, strain WB101^T had more numerous metabolic pathways, which explained why it had a relatively larger genome and demonstrated its potential application values.

Morphological, physiological, and biochemical characteristics

The cells of strain WB101^T were rod-shaped, 0.2–0.5 μm wide and 0.6–3.7 μm long after 3-day-growth in MB (Supplementary Fig. S2). The strain was Gram-stain-negative, oxidase-positive, catalase-positive, and could not motile on the surface of plate medium by flagella or gliding. Optimal growth occurred at 35–37°C (range 25–42°C), 5.0–6.0% (w/v) NaCl (range 1.0–11.0%), and pH 7.5–8.0 (range 7.0–8.5). There formed visible colonies on MA with or without 0.1% (w/v) KNO_3 in an anaerobic jar after three weeks. The nitrate reduction was negative, and no H_2S was detected by lead acetate papers or TSI.

Casein, Tweens 20, 40, 60, and 80 were hydrolysed by strain WB101^T, but DNA, alginate, starch, and carboxymethyl cellulose were not. It was susceptible to penicillin (10μg), ampicillin (10μg), carbenicillin (100μg), erythromycin (15μg), vancomycin (30μg), rifampicin (5μg), chloramphenicol (30μg), norfloxacin (30μg), ofloxacin (5μg), cefotaxime (30μg), clarithromycin (15μg), lincomycin (2μg), ceftriaxone (30μg), and polymyxin B (300μg), while resistant to tobramycin (10μg), tetracycline (30μg), neomycin (30μg), gentamycin (10μg), streptomycin (10μg), and kanamycin (30μg). Remarkably, according to available data of related taxa, including *Aliifodinibius salicampi* KHM44^T (Cho et al. 2017), '*Aliifodinibius salipaludis*' WN023^T (Zhao et al. 2020), *Aliifodinibius saliphilus* ECH52^T (Cho and Whang 2020), *Rhodohalobacter barkolensis* 15182^T (Han et al. 2018), and '*Rhodohalobacter mucosus*' 8A47^T, members in the phylum *Balneolota* showed the same sensitivity to vancomycin as strain WB101^T. However, vancomycin, a kind of glycopeptide antibiotics, is inherently inactive toward Gram-stain-negative bacterium because it cannot

cross the bacterial outer membrane (Yarlagadda et al. 2016). Thus, it suggested that cells of these taxa were different from typical Gram-stain-negative bacterium.

According to the API 20NE kits, strain WB101^T and three related strains were negative for nitrate reduction and indole production. Compared to *R. barkolensis* MCCC 1K03442^T and *R. halophilus* JZ3C29^T, strain WB101^T had a stronger positive reaction for assimilation of capric acid. Strain WB101^T showed positive activities for reactions of alkaline phosphatase, esterase (C4), esterase lipase (C8), leucine arylamidase, valine arylamidase, cystine arylamidase, trypsin, *α*-chymotrypsin, acid phosphatase, naphthol-AS-BI-phosphohydrolase, *α*-galactosidase (weakly), *β*-galactosidase, *β*-glucuronidase (weakly), *α*-glucosidase, *β*-glucosidase, *N*-acetyl-*β*-glucosaminidase, and *α*-mannosidase (weakly) in API ZYM kits. Positives for *β*-galactosidase and *N*-acetyl-*β*-glucosaminidase differentiated strain WB101^T from the three related type strains, and negatives for lipase (C14) and *α*-fucosidase was consistent in the genus *Rhodohalobacter*. The results of API 50CH indicated that acids were produced from d-arabinose, l-arabinose (weakly), d-ribose, d-xylose, l-xylose (weakly), d-glucose (weakly), d-fructose (weakly), d-mannose (weakly), l-sorbose, inositol, d-sorbitol, methyl-*α*d-mannopyranoside, *N*-acetyl glucosamine, arbutin, esculin ferric citrate, d-lyxose (weakly), d-tagatose, potassium 2-ketogluconate (weakly), and potassium 5-ketogluconate. Additionally, the positives for d-arabinose and d-sorbitol did not present in three related type strains. According to Biolog GEN III, strain WB101^T oxidized dextrin, d-maltose, d-trehalose, d-cellobiose, gentiobiose, sucrose, d-turanose, stachyose, d-raffinose, *α*- d-lactose, d-melibiose, *N*-acetyl-d-glucosamine, *N*-acetyl-d-galactosamine, *α*-d-glucose, d-mannose, d-galactose, d-fucose, l-histidine, pectin, d-galacturonic acid, l-galactonic acid lactone, d-glucuronic acid, glucuronamide, *α*-keto-glutaric acid, and acetoacetic acid. The oxidation of d-glucuronic acid and glucuronamide were stronger than others.

The further morphological, physiological, and biochemical characteristics that distinguish strain WB101^T from related type strains were summarized in Table 3.

Table 3
Characteristics that differentiate strain WB101T from related type strains.

Characteristic data	1	2	3	4
Oxygen requirement	Facultatively anaerobic	Aerobic [a]	Aerobic [b]	Facultatively anaerobic [c]
Temperature (°C)				
Growth range	25–42	20–42 [a]	10–40 [b]	20–50 [c]
Optimum	35–37	37–40 [a]	37 [b]	40 [c]
NaCl concentration (%, w/v)				
Growth range	1.0–11.0	2.0–14.0 [a]	0.5–4.0 [b]	2.0–16.0 [c]
Optimum	5.0–6.0	4.0–6.0 [a]	2.0–3.0 [b]	8.0–10.0 [c]
pH				
Growth range	7.0–8.5	7.0–9.0 [a]	7.0–8.0 [b]	7.0–9.0 [c]
Optimum	7.5–8.0	7.5–8.0 [a]	7.5 [b]	7.5–8.5 [c]
Hydrolysis of				
Starch	-	+ [a]	+ [b]	+ [c]
Casein	+	+ [a]	- [b]	ND [c]
Alginate	-	+ [a]	+ [b]	- [c]
Tweens 20	+	+ [a]	- [b]	- [c]
Tweens 40	+	- [a]	- [b]	- [c]
Tweens 60	+	- [a]	ND [b]	ND [c]
Tweens 80	+	- [a]	- [b]	- [c]

1, Strain WB101^T; 2, '*R. mucosus*' 8A47^T; 3, *R. barkolensis* MCCC 1K03442^T; 4, *R. halophilus* JZ3C29^T

+, positive; w, weakly positive; −, negative; ND, no data available

The data without particular indications are from this study

Data from: [a], Wang et al. (2021); [b], Han et al. (2018); [c], Xia et al. (2017)

Characteristic data	1	2	3	4
Acid production from				
d-Arabinose	+	-	-	-
Inositol	+	-	-	w
d-Sorbitol	+	-	-	-
Enzyme activities				
Oxidase	+	+[a]	-[b]	-[c]
β-Galactosidase	+	-	-	-
β-Glucosidase	+	+	-	-
N-Acetyl-*β*-glucosaminidase	+	-	-	-
Oxidation of				
d-Galactose	+	-	-	-
d-Fucose	+	-	-	-
Glycerol	-	-	+	+
Pectin	+	-	-	-
d-Glucuronic acid	+	-	-	w
1, Strain WB101^T; 2, '*R. mucosus*' 8A47^T; 3, *R. barkolensis* MCCC 1K03442^T; 4, *R. halophilus* JZ3C29^T				
+, positive; w, weakly positive; −, negative; ND, no data available				
The data without particular indications are from this study				
Data from: [a], Wang et al. (2021); [b], Han et al. (2018); [c], Xia et al. (2017)				

Chemotaxonomic analyses

The sole respiratory quinone of strain WB101^T was menaquinone 7 (MK-7), which was consistent with species of the genus *Rhodohalobacter*. Diphosphatidylglycerol (DPG), phosphatidylglycerol (PG), and phosphatidylcholine (PC) were the major polar lipids detected in strain WB101^T. In addition, moderate or minor amounts of phosphatidylethanolamine (PE), four unidentified lipids (L1, L2, L3, and L4), and three glycolipids (GL1, GL2, and GL3) were present. Compared to three related type strains, cells of strain WB101^T could synthesize lecithin, which was also identified in genomic analyses. The absence of aminolipid (AL1, AL2, and AL3) could differentiate strain WB101^T from '*R. mucosus*' 8A47^T and *R. barkolensis* MCCC 1K03442^T. Further details of the polar lipids content of strain WB101^T and three

related type strains were shown in Supplementary Fig. S3. High content of iso-$C_{15:0}$ was detected in strain WB101^T (53.8%), as well as the member of the genus *Rhodohalobacter*, which was considered as the major fatty acid (≥ 10.0%). As the minor fatty acids, $C_{12:0}$ and $C_{16:0}$ (≥ 1.0%, ≤ 10.0%) appeared in the cells of four strains. Detailed discrepancies between strain WB101^T and related type strains were listed in Supplementary Table S1.

Conclusions

Combined with the results of genotypic, phenotypic, and chemotaxonomic analyses, the similarities and differences between strain WB101^T and other related taxa were explicitly demonstrated. Based on the topologies of the phylogenetic and phylogenomic trees, we concluded strain WB101^T belongs to the genus *Rhodohalobacter* but differs from '*R. mucosus*', *R. barkolensis*, and *R. halophilus* at a novel species level. Therefore, *Rhodohalobacter sulfatireducens* sp. nov. is proposed, and strain WB101^T is the type strain.

Description of Rhodohalobacter sulfatireducens **sp. nov.**

Rhodohalobacter sulfatireducens (sul'fa'ti.re.du'cens. N.L. n. *sulfas -atis*, sulfate; L. v. *reducere* to lead back, bring back; N.L. part. adj. *sulfatireducens* reducing sulfate).

Cells are Gram-stain-negative, oxidase-positive, catalase-positive, non-motile, facultatively anaerobic, and rod-shaped (0.2–0.5 μm wide and 0.6–3.7 μm long). Colonies are reddish, convex, circular, and regular-edged on the MA plate. Growth occurs at 25–42°C (optimum, 35–37°C), 1.0–11.0% (w/v) NaCl (optimum, 5.0–6.0%), and pH 7.0–8.5 (optimum, 7.5–8.0). Hydrolysis of casein, Tweens 20, 40, 60, and 80 are positive. Negative for H_2S and indole productions. The activities of alkaline phosphatase, esterase (C4), esterase lipase (C8), leucine arylamidase, valine arylamidase, cystine arylamidase, trypsin, *α*-chymotrypsin, acid phosphatase, naphthol-AS-BI-phosphohydrolase, *α*-galactosidase (weakly), *β*-galactosidase, *β*-glucuronidase (weakly), *α*-glucosidase, *β*-glucosidase, *N*-acetyl-*β*-glucosaminidase, and *α*-mannosidase (weakly) are positive. Acids are produced from d-arabinose, l-arabinose (weakly), d-ribose, d-xylose, l-xylose (weakly), d-glucose (weakly), d-fructose (weakly), d-mannose (weakly), l-sorbose, inositol, d-sorbitol, methyl-*α*d-mannopyranoside, *N*-acetyl glucosamine, arbutin, esculin ferric citrate, d-lyxose (weakly), d-tagatose, potassium 2-ketogluconate (weakly), and potassium 5-ketogluconate. The carbon sources of dextrin, d-maltose, d-trehalose, d-cellobiose, gentiobiose, sucrose, d-turanose, stachyose, d-raffinose, *α*-d-lactose, d-melibiose, *N*-acetyl-d-glucosamine, *N*-acetyl-d-galactosamine, *α*-d-glucose, d-mannose, d-galactose, d-fucose, l-histidine, pectin, d-galacturonic acid, l-galactonic acid lactone, d-glucuronic acid, glucuronamide, *α*-keto-glutaric acid, and acetoacetic acid are oxidized. The sole respiratory quinone is MK-7. The polar lipid pattern consists of diphosphatidylglycerol (DPG), phosphatidylglycerol (PG), phosphatidylcholine (PC), phosphatidylethanolamine (PE), unidentified lipid (L), and glycolipids (GL). The major fatty acid is iso-$C_{15:0}$.

Type strain WB101^T (= KCTC 92204^T = MCCC 1H00518^T) was isolated from a marine solar saltern of Weihai, PR China. The genomic DNA G + C content is 42.0 mol%. The GenBank accession numbers are OM301685 for the 16S rRNA gene and JAKLWS000000000 for the draft genome.

Abbreviations

AAI, Average amino acid identity; ANI, Average nucleotide identity; ASR, Assimilatory sulfate reduction; BD, Becton Dickinson; dDDH, Digital DNA-DNA hybridization; GTDB, Genome Taxonomy Database; HPLC, High-performance liquid chromatography; KCTC, Korean Collection for Type Cultures; KEGG, Kyoto Encyclopedia of Genes and Genomes; LPSN, List of Prokaryotic names with Standing in Nomenclature; MA, Marine agar2216; MB, Marine broth 2216; MCCC, Marine Culture Collection of China; MEGA,Molecular Evolutionary Genetics Analysis; MIDI, Microbial Identification System; NCBI, National Centre of Biotechnology Information; NJ, Neighbour-joining; ML, Maximum-likelihood; MP, Maximum-parsimony; NRPS, Non-ribosomal peptide synthetase cluster; POCP, Percentage of conserved proteins; RAST, Rapid Annotationusing Subsystem Technology; TLC, Thin-layer chromatography; TSI, Triple-sugar iron agar.

Declarations

The GenBank accession number for the 16S rRNA gene sequence of *Rhodohalobacter sulfatireducens* WB101^T is OM301685, and the draft genome has been deposited at DDBJ/ENA/GenBank under the accession JAKLWS000000000.

Three supplementary figures and one supplementary table are available with the online version of this article.

Acknowledgements

This work of scanning electron microscope was supported by the Physical-Chemical Materials Analytical & Testing Centre of Shandong University at Weihai.

Funding

This work was supported by the National Natural Science Foundation of China (32070002) and the National Science and Technology Fundamental Resources Investigation Program of China (2019FY100700).

Conflicts of interests

The authors declare that they have no conflicts of interest.

Ethical statements

This article does not contain any studies with animals performed by any authors.

References

1. Aziz RK, Bartels D, Best AA et al (2008) The RAST Server: rapid annotations using subsystems technology. BMC Genomics 9:75
2. Bernardet JF, Nakagawa Y, Holmes B (2002) Proposed minimal standards for describing new taxa of the family *Flavobacteriaceae* and emended description of the family. Int J Syst Evol Microbiol 52:1049–1070
3. Bowman JP (2000) Description of *Cellulophaga algicola* sp. nov., isolated from the surfaces of Antarctic algae, and reclassification of *Cytophaga uliginosa* (ZoBell and Upham 1944) Reichenbach 1989 as *Cellulophaga uliginosa* comb. nov. Int J Syst Evol Microbiol 50:1861–1868
4. Buyer JS (2002) Rapid sample processing and fast gas chromatography for identification of bacteria by fatty acid analysis. J Microbiol Methods 51:209–215
5. Carbonero F, Benefiel AC, Alizadeh-Ghamsari AH, Gaskins HR (2012) Microbial pathways in colonic sulfur metabolism and links with health and disease. Front Physiol 3:448
6. Chaumeil PA, Mussig AJ, Hugenholtz P, Parks DH (2019) GTDB-Tk: a toolkit to classify genomes with the Genome Taxonomy Database. Bioinformatics 36:1925–1927
7. Cho GY, Lee JC, Whang KS (2017) *Aliifodinibius salicampi* sp. nov., a moderately halophilic bacterium isolated from a grey saltern. Int J Syst Evol Microbiol 67:2598–2603
8. Cho GY, Whang KS (2020) *Aliifodinibius saliphilus* sp. nov., a moderately halophilic bacterium isolated from sediment of a crystallizing pond of a saltern. Int J Syst Evol Microbiol 70:358–363
9. CLSI (2012) Performance standards for antimicrobial susceptibility testing, twenty-second informational supplement CLSI document M100–S22. Clinical and Laboratory Standards Institute, Wayne
10. Cowan ST, Steel KJ (1974) Bacterial characters and characterization, 2nd edn. Cambridge University Press, Cambridge
11. Felsenstein J (1981) Evolutionary trees from DNA sequences: a maximum likelihood approach. J Mol Evol 17:368–376
12. Fitch WM (1971) Toward defining the course of evolution: minimum change for a specific tree Topology. Syst Zool 20:406–416
13. Han SB, Yu YH, Ju Z, Li Y, Zhang R, Hou XJ, Ma XY, Yu XY, Sun C, Wu M (2018) *Rhodohalobacter barkolensis* sp. nov., isolated from a saline lake and emended description of the genus *Rhodohalobacter*. Int J Syst Evol Microbiol 68:1949–1954
14. Kanehisa M, Sato Y, Kawashima M, Furumichi M, Tanabe M (2016) KEGG as a reference resource for gene and protein annotation. Nucleic Acids Res 44:D457–D462

15. Kim OS, Cho YJ, Lee K et al (2012) Introducing EzTaxon-e: a prokaryotic 16S rRNA gene sequence database with phylotypes that represent uncultured species. Int J Syst Evol 62:716–721
16. Kimura M (1980) A simple method for estimating evolutionary rates of base substitutions through comparative studies of nucleotide sequences. J Mol Evol 16:111–120
17. Kroppenstedt RM (1982) Separation of bacterial menaquinones by HPLC using reverse phase (RP18) and a silver loaded ion exchanger as stationary phases. J Liq Chromatogr 5:2359–2367
18. Kumar S, Stecher G, Tamura K (2016) MEGA7: molecular evolutionary genetics analysis version 7.0 for bigger datasets. Mol Biol Evol 33:1870–1874
19. Kushkevych I, Cejnar J, Treml J, Dordević D, Kollar P, Vítězová M (2020) Recent advances in metabolic pathways of sulfate reduction in intestinal bacteria. Cells 9:698
20. Li R, Zhu H, Ruan J et al (2010) Denovo assembly of human genomes with massively parallel short read sequencing. Genome Res 20:265–272
21. Liu QQ, Wang Y, Li J, Du ZJ, Chen GJ (2014) *Saccharicrinis carchari* sp. nov., isolated from a shark, and emended descriptions of the genus *Saccharicrinis* and *Saccharicrinis fermentans*. Int J Syst Evol Microbiol 64:2204–2209
22. Ma K, Weiss R, Adams MW (2000) Characterization of hydrogenase II from the hyperthermophilic archaeon Pyrococcus furiosus and assessment of its role in sulfur reduction. J Bacteriol 182:1864–1871
23. Medema MH, Blin K, Cimermancic P et al (2011) antiSMASH: rapid identification, annotation and analysis of secondary metabolite biosynthesis gene clusters in bacterial and fungal genome sequences. Nucleic Acids Res 39:W339–W346
24. Meier-Kolthoff JP, Carbasse JS, Peinado-Olarte RL, Göker M (2022) TYGS and LPSN: a database tandem for fast and reliable genome-based classification and nomenclature of prokaryotes. Nucleic Acid Res 50:D801–D807
25. Qin QL, Xie BB, Zhang XY, Chen XL, Zhou BC, Zhou J, Oren A, Zhang YZ (2014) A proposed genus boundary for the prokaryotes based on genomic insights. J Bacteriol 196:2210–2215
26. Richter M, Rosselló-Móra R (2009) Shifting the genomic gold standard for the prokaryotic species definition. Proc Natl Acad Sci USA 106:19126–19131
27. Richter M, Rosselló-Móra R, Oliver Glöckner F, Peplies J (2016) JSpeciesWS: a web server for prokaryotic species circumscription based on pairwise genome comparison. Bioinformatics 32:929–931
28. Rodriguez -RLM, Konstantinidis KT (2014) Bypassing cultivation to identify bacterial species. Microbe Mag 9:111–118
29. Saitou N, Nei M (1987) The neighbor-joining method: a new method for reconstructing phylogenetic trees. Mol Biol Evol 4:406–425
30. Schiff JA (1979) Pathways of assimilatory sulphate reduction in plants and microorganisms. Ciba Found. Symp. 72:49–69

31. Simpson JT, Wong K, Jackman SD, Schein JE, Jones SJ, Birol I (2009) ABySS: a parallel assembler for short read sequence data. Genome Res 19:1117–1123
32. Smibert RM, Krieg NR (1994) Phenotypic characterization. In: Gerhardt P, Murray RGE, Wood WA, Krieg NR (eds) Methods for general and molecular bacteriology. American Society For Microbiology, Washington, pp 611–651
33. Tindall BJ, Sikorski J, Smibert RA, Krieg NR (2007) Phenotypic characterization and the principles of comparative systematics. Methods for General and Molecular Microbiology, Third Edition. American Society for Microbiology, Washington, DC, pp 330–393
34. Wang TJ, Liu ZW, Feng X, Zou QH, Du ZJ (2021) *Rhodohalobacter mucosus* sp. nov., isolated from a marine solar saltern. Arch Microbiol 203:2419–2424
35. Wang YX, Liu JH, Xiao W, Zhang XX, Li YQ, Lai YH, Ji KY, Wen ML, Cui XL (2012) *Fodinibius salinus* gen. nov., sp. nov., a moderately halophilic bacterium isolated from a salt mine. Int J Syst Evol Microbiol 62:390–396
36. Xia J, Ling SK, Wang XQ, Chen GJ, Du ZJ (2016) *Aliifodinibius halophilus* sp. nov., a moderately halophilic member of the genus *Aliifodinibius*, and proposal of *Balneolaceae* fam. nov. Int J Syst Evol Microbiol 66:2225–2233
37. Xia J, Xie ZH, Dunlap CA, Rooney AP, Du ZJ (2017) *Rhodohalobacter halophilus* gen. nov., sp. nov., a moderately halophilic member of the family *Balneolaceae*. Int J Syst Evol Microbiol 67:1281–1287
38. Yarlagadda V, Manjunath GB, Sarkar P et al (2016) Glycopeptide antibiotic to overcome the intrinsic resistance of Gram-negative bacteria. ACS Infect Dis 2:132–139
39. Yoon SH, Ha SM, Lim J, Kwon S, Chun J (2017) A large-scale evaluation of algorithms to calculate average nucleotide identity. Antonie Van Leeuwenhoek 110:1281–1286
40. Zhao X, Miao S, Sun Y, Gong Q, Zhao J, Wang J, Zhang G (2020) *Aliifodinibius salipaludis* sp. nov., Isolated from Saline-Alkaline Soil. Curr Microbiol 77:1328–1333

Figures

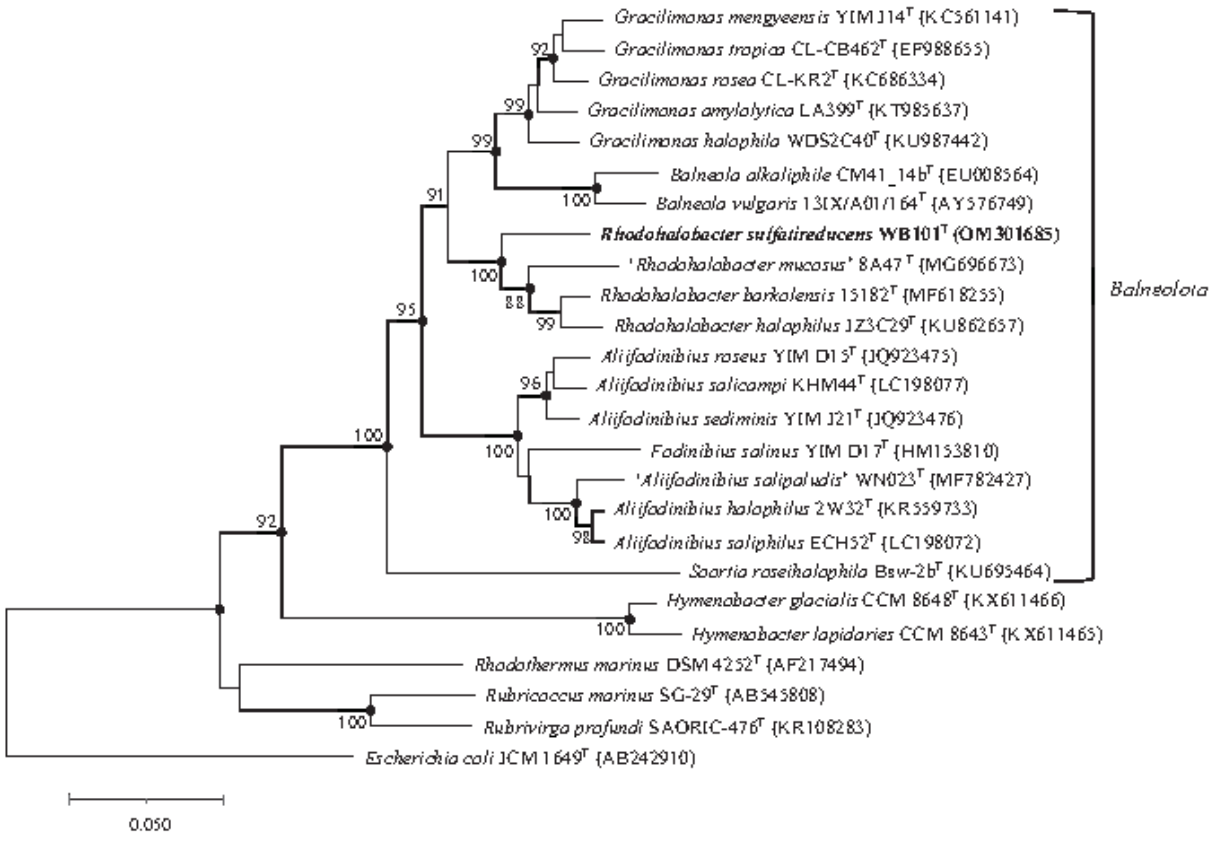

Figure 1

Neighbour-joining phylogenetic tree constructed from the 16S rRNA gene sequences, showing the position of strain WB101^T and related taxa within the phylum *Balneolota* and others. Percentage bootstrap values (1,000 replications) greater than 70 % are shown at branch points. The filled circles indicate that the corresponding nodes were also confidently found in the trees by the maximum-likelihood and maximum-parsimony algorithms. GenBank accession numbers of the 16S rRNA gene sequences are given in parentheses. *Escherichia coli* JCM 1649^T (AB242910) was used as an outgroup. Bar, 0.05 substitutions per nucleotide position.

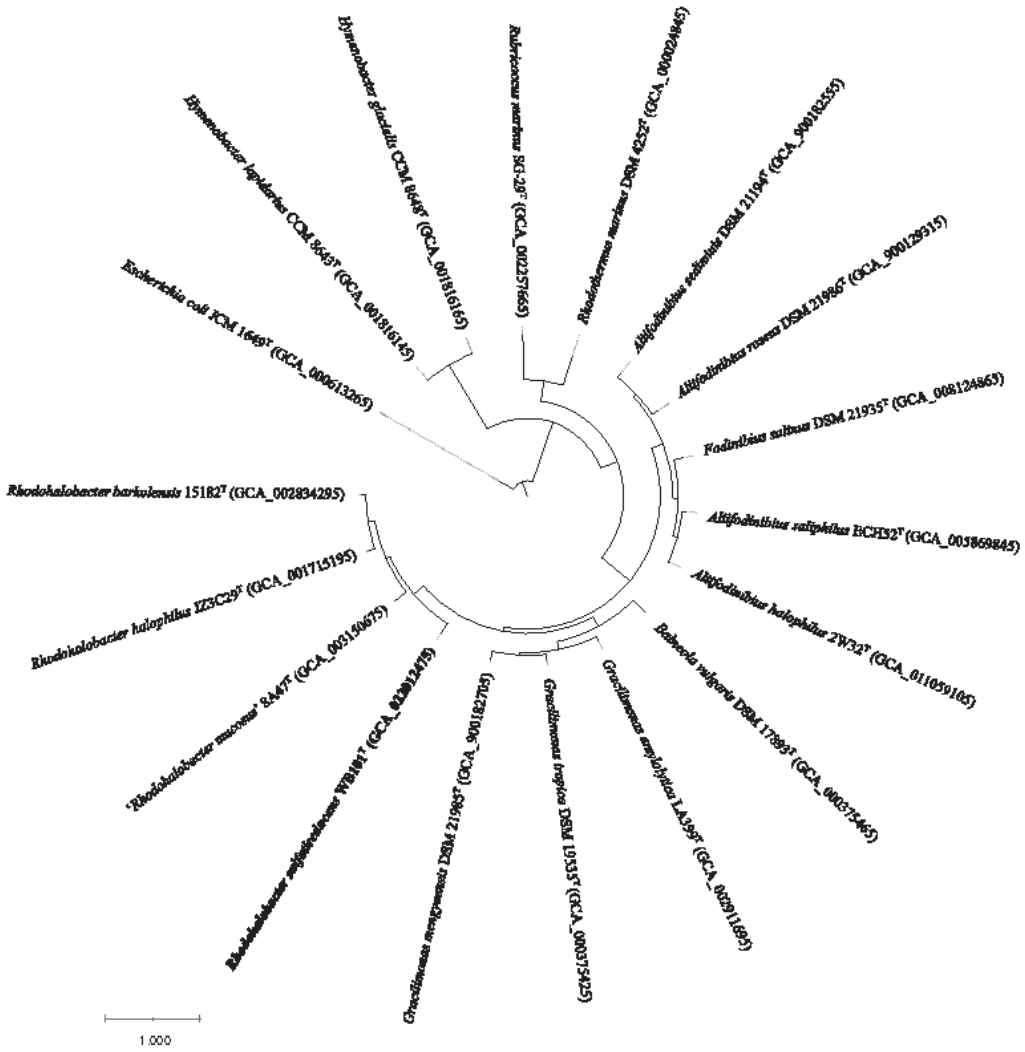

Figure 2

Maximum-likelihood phylogenomic trees based on genomes inferred the bac120 marker set of strain WB101^T and related taxa within the phylum *Balneolota* and others. GenBank accession numbers of assemblies are given in parentheses. *Escherichia coli* JCM 1649^T (GCA_000613265) was used as an outgroup. Bar, 1.0 substitutions per nucleotide position.

Supplementary Files

This is a list of supplementary files associated with this preprint. Click to download.

- WB101supplementarymaterials.docx